Sustainable Engineering Materials
ISSN: 3105-1960 (Print); ISSN: 3105-1979 (Online)
http://www.sustain-dpl.com/picnews.asp?id=177
DOI: 10.54113/j.suem.2026.000016

ORIGINAL ARTICLE

Unveiling the impact of steel fiber type on self-compacting concrete performance under intense fire

Hadeel K Awad, Rawaa K Aboud*, Zaid S.Aljoumaily, Mohamed Z.Al-mulali

Civil Engineering Department, College of engineering, University of Baghdad, Baghdad, Iraq
*Corresponding Author: Rawaa K Aboud. Email: rawaa.khalid@coeng.uobaghdad.edu.iq

Abstract: One of the problems that concrete structures may face is fire exposure, which can cause several issues for concrete structures, deterioration, reduction in serviceability, and potentially demolition. In this study, self-compacting concrete was used and reinforced with steel fiber as a volume fraction V_f by 0.75, 1.25, and 1.75% for both hook and micro steel fiber. The fresh and mechanical properties of all the tested mixes were examined. It was observed that the addition of fibers reduced the fresh properties and increased the mechanical properties for both types of fibers, especially for hook steel fiber. To study the effect of fire exposure on the properties of concrete, the samples were subjected to direct burning at temperatures reaching 300, 400, and 500°C for one hour of exposure, followed by gradual cooling to ambient temperature. It was noted that the mechanical properties significantly decreased with increasing burning temperatures, and the presence of fibers mitigated the deterioration that concrete is subjected to during burning. This enhancement was directly proportional to the augmentation of fiber volume fraction for both types, except for 1.75% hook steel fiber at 400 and 500°C, where there was a decrease in the improvement rates. Moreover, as for 1.75% micro steel fibers, this behavior was observed at 500°C only.

Keywords: self-compacting concrete, hook steel fiber, micro steel fiber, percentage volume fraction, fire flame, and mechanical properties

1 Introduction

Fire is concerned as one of the most severe risks on concrete structures. When concrete is exposed to high temperatures during a fire, it can suffer significant damage, including cracking, spalling, and a reduction in strength [1-4]. These effects not only weaken the structure but can also make it unsafe for use afterwards. As buildings become more complex and safety standards more demanding, understanding how different types of concrete behave under fire conditions is increasingly important [5-8]. Although conventional concrete has been the subject of extensive research regarding its behavior under fire exposure, comparatively less attention has been given to advanced materials such as Self-Compacting Concrete (SCC) [9-12]. SCC is an innovative type of concrete characterized by its ability to flow under its own weight and fully consolidate without the need for external vibration, enabling it to fill complex formwork and encapsulate dense reinforcement [13-16]. This self-compacting capability is achieved through a carefully proportioned mix that typically incorporates a higher content of fine materials, chemical admixtures, and, in many cases, supplementary

Received: 18 November 2024; Received in revised form: 25 March 2026; Accepted: 8 May 2026

cementitious materials such as fly ash or ground granulated blast furnace slag.[17] While these modifications enhance the workability, uniformity, and mechanical performance of SCC, they also introduce uncertainties regarding the material's response to elevated temperatures [18, 19]. Because of its different composition and behavior, SCC may respond to fire in ways that differ from conventional concrete. Its dense structure, while beneficial for strength and durability, can also trap moisture, which increases the risk of explosive spalling under high temperatures [20, 21].

The utilization of fiber enhances the mechanical characteristics of SCC and restrains the development of cracks. However, these improvements vary and depend on fiber type, and the percentage of volume fraction, [22-25]. Moreover, the workability, aggregate particles size and fiber percentage should be taken into consideration when utilizing fiber in self-compacting concrete. Using a single fiber type enhances the properties of concrete at a restricted level, unlike the utilization of more than one type of fiber in which it enhances the properties of concrete even further [26,27]. Increased strength and toughness were noticed when using a combination of macro-fiber (0.5mm in diameter) and micro-fiber (less than 0.022 mm in diameter) when studying failure processes at different stages for concrete. Adding steel fibers helps improve concrete resistance to cracking and helps it retain strength after exposure to fire. However, unlike polypropylene fibers, steel fibers are less effective at relieving internal vapor pressure, so their reduction of the occurrence of spalling is insignificant. Even so, their contribution to maintaining the structural integrity of SCC under fire conditions is well recognized [28, 29]. The effect of burning at temperatures at (300, 400, and 500) ^{O}C on high-performance concrete (HPC) was studied, and its impact on some mechanical properties after reinforcement with steel fibers for two burning durations (1 and 1.5 hour) was examined. It was concluded that the compressive strength decreased with the increased of exposure burning duration and also with higher burning temperatures, where the residual strength was between 36-78% for reference mix and between 49-89% for fiber-reinforced concrete [30]. In another study, the effect of steel fibers on the microstructure and toughness of concrete exposed to high temperatures of 500 ^{O}C was examined. The study showed that adding fibers increases the resistance to bending and splitting and reduces the loss occurring after exposure to fire. On the other hand, concrete without fibers was more sensitive and deteriorated more than concrete with steel fibers. As for the toughness test, the presence of fibers reduced the deterioration caused by burning, with an increase in toughness by 600-800% compared to the concrete without fibers [31]. Other research found that adding steel fiber with (0.25 and 0.5) % and polypropylene fiber of (0.15) % as volume percentages to lightweight self-compacting concrete exposed to burning at temperatures of (300, 450, and 600) OC, improved the compressive strength, splitting tensile strength, and ultrasonic pulse velocity, especially at burning temperatures of (450 and 600) OC [32]. The addition of micro steel fibers in proportions (0.5, 1, and 1.5) % as a volumetric ratio had an impact on the behavior of reactive powder concrete exposed to burning temperatures of (300, 400, and 500) OC. The results showed that the reference mix (without fibers) yielded the worst results in the approved tests compared to the fiber-containing mixes for all burning temperatures, especially at 500 OC. The 1.5% fiber content improved the properties at 300 OC by (6.67, 4.13, and 7)% for compressive, splitting, and flexural strengths, respectively [33]. This study investigates the influence of different types of steel fibers specifically hooked and micro steel fibers—incorporated at varying volume fractions (0%, 0.75%, 1.25%, and 1.75%) on the mechanical properties of self-compacting concrete (SCC) subjected to fire flame at different temperatures (ambient, 300 °C, 400 °C, and 500 °C). The specimens were cooled (quenching) using gradual cooling method to assess the combined effects of fiber type, dosage, and fire exposure on SCC performance. The study of steel fiber-reinforced self-compacting concrete (SCC) under the influence of high temperatures or fire is of great importance due to the increasing use of this type of concrete in modern structures such as high-rise buildings, bridges, and complex reinforcement structures. Although self-compacting concrete (SCC) is characterized by high workability and good density, exposure to high temperatures may lead to deterioration in its microstructure, increased porosity, and the formation of micro-cracks, which negatively affects its mechanical performance. This research aims to explore how different steel fiber types, added in varying amounts, influence the strength and durability of self-compacting concrete after being exposed fire flame at different temperatures with gradual cooling method, the study seeks to understand how these combined factors affect the concrete’s

performance and to determine which fiber configurations offer the best protection under fire conditions.

2 Materials

Self-compacting concrete employed for this study consists of many main components to inshore a designed compressive strength of ($f_c' \approx 45$ MPa). Ordinary Portland cement OPC (CEM I 42.5 N), according to the IQS 5/ 2019 [34], and type I according to ASTM C150/C150M-20 [35] specifications, was used. **Tab. 1** displays the chemical composition and main compounds for (OPC), while the physical properties are illustrated in **Tab. 2**. A Nominal size of (10) mm coarse aggregate conforming to the requirements of IQS 45/1984 [36], and Nominal size (9.5-2.36) according to ASTM C33/C33M-18 [32] was utilized; sieve analysis, and physical with chemical characteristics for coarse aggregate are presented in **Tab. 3** and **Tab. 4**, respectively. Fine aggregate classified as zone 2 according to IQS 45/1984[36], and fulfills ASTM C33/C33M-18[37] was used, physical and chemical properties, and sieve analysis; are displayed in **Tab. 5** and **Tab. 6**, respectively. The additive material applied in this study was silica fume by 3% as a partial replacement by weight of cement, which conforms to ASTM C1240-20 [38] with accelerated pozzolanic strength activity index at 7 days of 115%. Physical properties and chemical analysis of silica fume are illustrated in **Tab. 7** and **Tab. 8**, respectively. To enhance SCC workability Super-Plasticizer, type F was utilized conforming ASTM C494/ C494M-17 [39]. Technical properties for the super-plasticizer used are listed in **Tab. 9**. Two types of steel fibers, micro steel fiber and hooked steel fiber, were adopted, as shown in **Fig. 1**. The Properties of the steel fibers are illustrated in **Tab. 10.**

Table 1. Chemical Composition and Main Compounds of OPC

Chemical Composition	Result	IQS No. 5/2019 Limits	ASTM C150-20 Limits/ type I
Lime (CaO)	63.4	-----	-----
Silica (SiO_2)	22.1	-----	-----
Alumina ($Al2O_3$)	3.72	-----	-----
Iron Oxide ($Fe2O_3$)	2.41	-----	-----
Magnesia (MgO)	3.82	≤5.0	≤6.0 %
Sulfate (SO_3)	2.53	≤ 2.8 If C_3A > 3.5	≤3.0 if C_3A≤8%
Insoluble residue (I.R)	0.86	≤1.5	≤1.5 %
Loss on Ignition (L.O.I)	1.13	≤4.0	≤3.0 %
	Main Compound of OPC		
Tri Calcium Silicate (C_3S)	54.42		
Di Calcium Silicate (C_2S)	22.39		
Tri Calcium Aluminate (C_3A)	5.78		
Tera Calcium Aluminate Ferrite (C_4AF)	7.32		

Table 2. Physical Properties of OPC

Physical Properties		Result	IQS No. 5/2019 Limits		ASTM C150-20 Limits/ type I
Specific surface area m^2/kg (Blain method)		334	≥ 250		≥ 260
Initial setting time, (min)		131	≥ 45		≥ 45 min
Final setting time, (hr.: min)		5:14	≤ 10		≤375min
Compressive strength, (MPa)	@ 2 day	19	≥ 10	@ 3 day	≥ 12
	@ 28 day	42.8	≥ 42.5	@ 7 day	≥ 19

Table 4. Chemical and physical properties of coarse aggregate

Property	Test Result	IQS No. 45/1984Limits
Specific gravity	2.61	------
Absorption	0.9%	------
Sulfate content (SO_3)	0.06%	≤0.1%
Dry rodded density kg/m3	1602	------

Table 3. Sieve analysis of coarse aggregate

Sieve size (mm)	Passing %	IQS No. 45/1984Limits Nominal size (10) mm	Limits of ASTM C33-18 Nominal size (9.5-2.36)
14	100	100	-
12.5	100	-	100
10	93	85-100	85-100
4.75	20	0-25	10-30
2.36	2	0-5	0-10

Table 5. Chemical and Physical Properties of Fine Aggregate

Property	Specification	Result	IQS No. 45/1984Limits
Specific gravity	ASTM C128	2.58	--------
Absorption	ASTM C128	0.94%	--------
Dry rodded density	ASTM C29/C29M	1638kg/m3	--------
Sulfate content SO_3	Iraqi Reference Guide No.500/3, 2018	0.37%	≤0.5%
Fine particles passing from sieve 75 µm	Iraqi Reference Guide No.500/4, 2018	3.18%	≤5.0%

Table 6. Sieve analysis of Fine Aggregate

Sieve size (mm)	Passing %	IQS No. 45/1984Limits - zone (2)	Limits of ASTM C33-18
10	100	100	100
4.75	95	90-100	95-100
2.36	80	75-90	80-100
1.18	69	55-90	50-85
0.6	51	35-59	25-60
0.3	22	8-30	5-30
0.15	3	0-10	0-10
0.075	0		0-3

Table 7. Physical Properties for Silica Fume

Physical Properties	Result	ASTM C1240-20
Percent retained on 45-µm (No.325) sieve	6%	≤ 10
Accelerated pozzolanic Strength activity index @ 7 days	115 %	≥ 105
Specific surface area	18 m^2/gm	≥ 15

Table 8. Chemical Analysis for Silica Fume

Oxide composition	Oxide content %	ASTM C1240-20
SiO_2	90.9	≥ 85.0
Al_2O_3	0.36	----
Fe_2O_3	1.22	----
CaO	1.8	----
SO_3	0.56	----
MgO	2.21	----
Na_2O	0.17	----
K_2O	0.09	----
L.O. I	2.2	≤ 6.0
Moisture content	0.4	≤ 3.0

Table 9. Technical Properties for Super-Plasticizer

Appearance	Transparent or Light Brown Liquid
Calcium Chloride	Nil
Density	1.10 ± 0.02 gm/ml
Viscosity	450 cPs @ 20°C
Setting time	Initial and final setting time depends on temperature, cement quantity and dosage used
Packaging	Packed in 20-liter Jerrycans or 1000-liter IBCs

* Manufacturers data

Table 10. Steel Fibers Properties

Appearance		Hook steel fiber	Micro steel fiber
Length	(mm)	35	13
Diameter	(mm)	0.55	0.2
Aspect ratio	(l/d)	64	60
Tensile Strength	(MPa)	2200	≥ 2850
Density	(kg/m^3)	7800	7850

* Manufacturers data

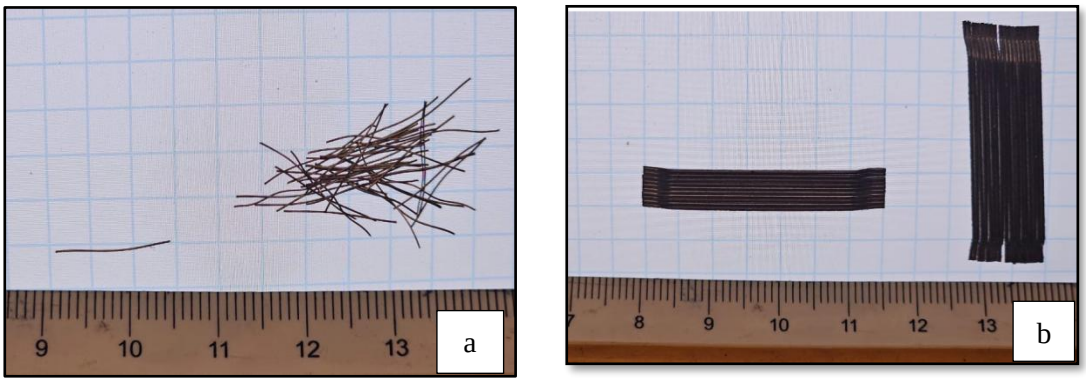

Fig.1. steel fibers: a-micro steel fiber, b- hooked steel fiber.

3 Mix proportions

Several trial mixes were conducted before starting the main mix to achieve the desired workability according to EFNARC, 2005 [40] and the designed strength. Seven mixes had been prepared with a fixed amount of w/c ratio, silica fume and water reducing agent. As mentioned earlier, the research intends to investigate two types of steel fibers with different percentages of volume fractions (V_f %) as 0.75% up to 1.75% with increments of 0.5% in self-compacting concrete and exposed to fire ranging in temperature between 300 to 500°C. **Tab. 11** lists the constituents for the prepared mixes.

Tab. 11. Mix proportions for SCCmixes

Mixes	Cement kg/m^3	Silica Fume kg/m^3	Sand kg/m^3	Gravel kg/m^3	Water kg/m^3	Micro steel fiber V_f %	Hooked steel fiber V_f %
MR	557	16.7	755	879	172.1	0	0
MS0.75	557	16.7	755	879	172.1	0.75	0
MS1.25	557	16.7	755	879	172.1	1.25	0
MS1.75	557	16.7	755	879	172.1	1.75	0
MH0.75	557	16.7	755	879	172.1	0	0.75
MH1.25	557	16.7	755	879	172.1	0	1.25
MH1.75	557	16.7	755	879	172.1	0	1.75

SP = 0.9 l /100 kg of cement / Silica fume = 3% replacement by cement weight / w/p = 0.3

4 Testing method and discussion

4.1 Fresh properties

The main characteristic of self-compacting concrete is its high workability without segregation easing the process of concreting filling up densely reinforced formwork. Hence, slump flow, T_{500} (filling capacity), V funnel (viscosity) and L-box test (passing ability) were conducted in accordance with the European guideline and many researches [11,12][40-43]. Also, for segregation characteristics, the sieve-segregation index test is investigated.

The fresh properties of SCC and the effect of both types of fibers (micro steel and hooked end) on the workability of fresh SCC samples were conducted, as shown in **Tab. 12**.

Table 12. Fresh Properties of SCC mixes

Mixes	Slump flow (mm)	T_{500mm} (sec)	V-funnel (sec)	L-box	Segregation index, %
MR	776	3.6	9.3	0.94	13.9
MS0.75	744	4.7	10.1	0.91	12.2
MS1.25	715	5.5	11.4	0.89	10.5
MS1.75	688	6.3	12.5	0.82	9.1
MH0.75	723	5.2	10.8	0.89	11.5
MH1.25	691	6.1	12.1	0.85	9.6
MH1.75	657	7.7	14.3	0.81	8.1
(EFNARC, 2005) Limits	SF1 550 - 650 SF2 660 - 750 SF3 760 - 850	$T_{500} > 2$, V-funnel (9 to 25)	≥ 0.8		SR1 ≤ 20 SR2 ≤ 15

4.1.1 Slump and T_{500mm} tests

The results of slump test for the SCC mixes containing both types of fiber are shown in **Fig.2**. As a general observation, the increase in volume of any types of fiber reduced the workability of the mix proportionally [44]. In comparison to the control mix, SCC mixes containing micro steel fiber showed a reduction in slump reaching 11.34**%** at the volume fraction of 1.75%. However, the reduction in slump readings exhibited by SCC mixes containing hooked end fiber was higher in comparison to their micro-steel counterparts at all volume fraction percentages [30]. At the volume fraction of 1.75% of hooked end fiber, the slump of SCC mixes was reduced to 15.3% in compared to the control mix. This is due to the differences in surface area, geometry and the interaction of these different types of fiber with the fresh mix. Hooked end fiber anchor themselves mechanically into the mix leading the SCC mix to resist flow. In addition, the higher surface area of bonding that hooked end fiber possesses increases the friction, hence, reducing the flow of the mix.

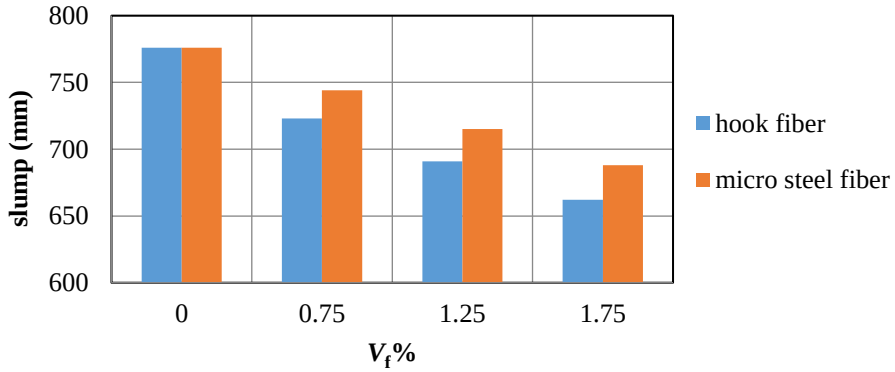

Fig. 2. Effect of micro and hook steel fiber on slump test

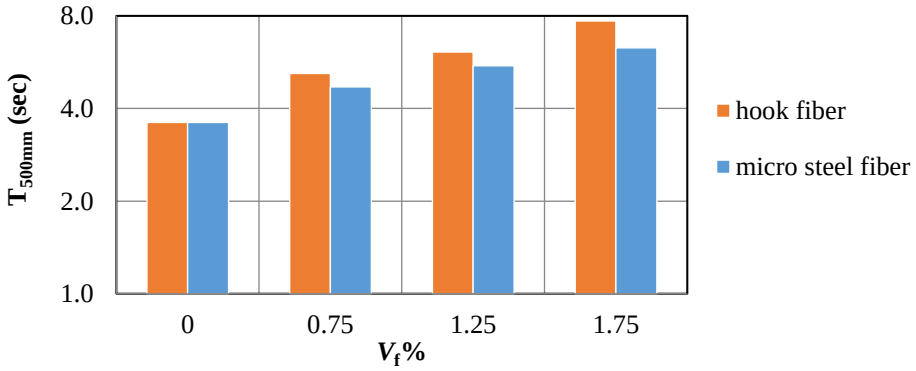

Fig. 3. Effect of micro and hook steel fiber on T_{500} test

Concerning to T_{500mm} test, micro-steel fiber SCC mixes showed times lower in comparison to SCC mixes containing hooked end fiber at similar volume fractions as shown in **Fig.3**. Mixes containing micro steel fiber exhibited times of 4.7, 5.5 and 6.3 seconds at volume fractions of 0.75, 1.25 and 1.75% respectively. Whereas hooked end SCC mixes exhibited times of 5.2, 6.1 and 7.7

seconds at similar volume fractions. The increase in time that SCC mixes containing hooked end fiber to complete the T_{500mm} test is due to longer length and larger diameter that this fiber has in comparison to that of the micro-steel fiber. Longer fiber tends to experience more entanglement with each other during flow leading to resisting the movement of the mix.

4.1.2 V-funnel test

This test investigates the mix's overall flow through a narrow opening. However, this test has a higher sensitivity towards blocking or fiber interlocking in comparison to the T_{500mm}. Increased times were exhibited by SCC mixes containing fiber regardless of fiber type as shown in **Fig.4**. SCC mixes containing hooked end fiber showed increased time readings in comparison to their micro-steel fiber counterparts at the same volume fractions. SCC mixes containing hooked end fiber showed higher time readings that reached 14.3 seconds at a volume fraction of 1.75%. In comparison to SCC mixes containing micro-steel fiber, at a similar volume fraction, the V-funnel reading was 12.5 seconds. Therefore, a similar trend was exhibited as the T_{500mm} test. This is compatible with the fact that hooked end fiber may interlock on each other or with the coarse aggregate inside the funnel leading to highly viscous mix leading to the reduction of passing ability.

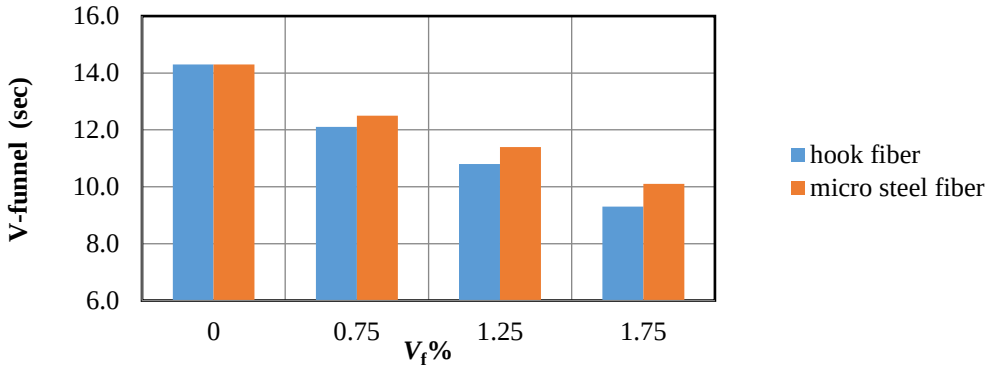

Fig. 4. Effect of micro and hook steel fiber on V-funnel test

4.1.3 L-box test

To ensure that SCC mixes can flow through congested reinforcement, the L-box test is crucial for passing ability. **Fig.5** shows the L-box test behavior for the control and SCC mixes containing micro-steel and hooked end fibers. Regardless of fiber type, SCC mixes containing fiber showed lower L-box readings than that exhibited by the control SCC mix and the higher volume fraction of fiber in the SCC mix leads to a lower L-box reading. When comparing SCC mixes containing both types of fiber, micro-steel fiber SCC mixes show a higher passing ability reading than those exhibited by hooked end SCC mixes with similar volume fractions. Micro steel fiber SCC mixes exhibited readings ranging from 0.91 to 0.82. While hook end SCC mixes showed readings ranging from 0.89 to 0.81. The possibility of fiber bridging in SCC mixes containing micro-steel fiber is lower than that of SCC mixes containing hooked end fiber. This is caused by the lower mechanical interlocking of micro-steel fibers and to their shorter and thinner geometry. It is known that the thicker longer hooked end fiber has a high tendency to entanglement leading to the restriction of movement.

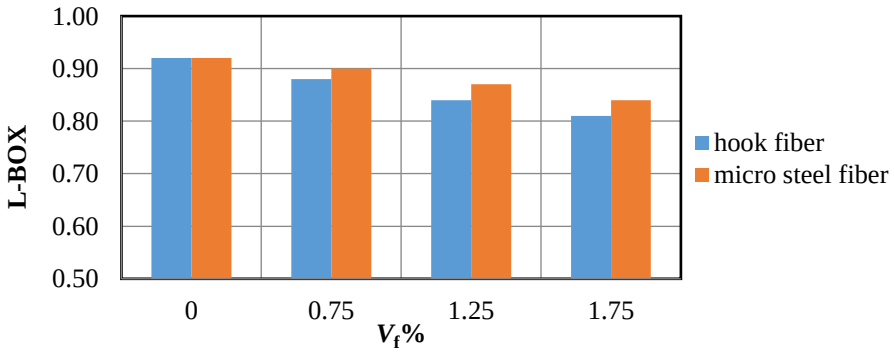

Fig. 5. Effect of micro and hook steel fiber on L-box test

4.1.4 Segregation index test

The sieve-segregation index test according to **Tab. 12**, it was observed that all mixes fall within the EFNARC (2005) specifications and are classified as (SR2). However, it was noted, according to **Fig.6**, that the effect of the fibers is inversely proportional to the segregation index for both types of fibers and for various percentages used. The reduction percentage reached to (34.5, 41.7) % for the two types of steel fibers (micro and hook) used with 1.75 volume fractions, respectively. The addition of hook type fiber had the most significant effect compared to micro type fiber, for the same volume fractions the reduction percentage reached 10.9% due to the fiber length and the interlocking of hook type fibers within the mixes.

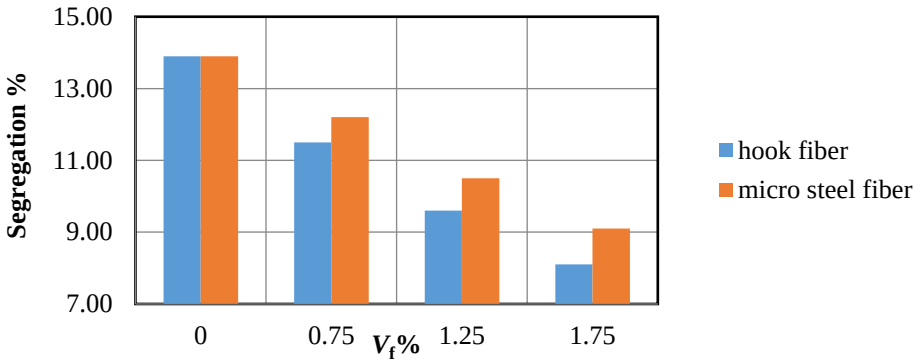

Fig. 6. Effect of micro and hook steel fiber on segregation index test

4.2 Hardened properties

A total of 252 specimens were casted and prepared. A cubic specimen of 100mm for compressive strength, cylinders having the dimensions of 100mm in diameter and 200mm in length for splitting tensile strength, and prisms of (75×75×380) mm for flexural strength. Samples were demolded after 24 hours and immersed in water up to the age of 28days ASTM C192/C192M-24 [45]. However for fire flam exposure 187 specimens were kept in laboratory conditions, in terms of temperature and humidity, for another 28 days allowing the specimens to dry out completely and prevent any moisture from existing within the specimens' core. This is done to prevent the occurrence of internal stresses when these samples are subjected to high temperatures causing the specimens to spall [3] [7].

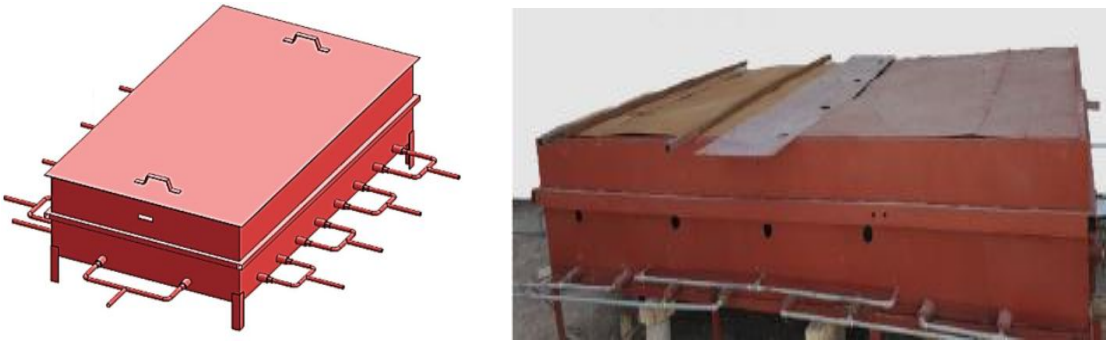

Fig. 7. Burning furnace

Fig. 8. Digital thermometer

Specimens were subjected to fire using a steel furnace having the dimensions of (3000×1350×500) mm as shown in **Fig.7**, with constant-steady burning temperatures of (300, 400 and 500) °C using a thermocouple as demonstrated in **Fig. 8**, The selected burn degrees were achieved based on ASTM E119 [46]. Cooling procedures were implemented on the specimens to replicate the thermal response of structural elements subjected to fire exposure.

4.2.1 Compressive Strength

This test was conducted according to BS EN 12390-3:2019 [47]. At standard ambient temperature (25°C), the compressive strength results indicated that increasing the fiber volume fraction led to higher compressive strength, particularly with hooked steel fibers as illustrated in **Tab. 13**. **Fig. 9 (a, and b)** shows the compressive strength results for micro and hook steel fibers at ambient and different burning temperatures.

Table 13. Compressive strength results at different burning temperatures using micro and hook steel fibers

Compressive strength (MPa)								
	Micro steel fiber				Hook steel fiber			
Temp. °C	MR	MS0.75	MS1.25	MS1.75	MR	MH0.75	MH1.25	MH1.75
25	48.00	49.70	52.80	53.4	48.00	50.64	54.24	55.87
300	39.90	41.84	45.83	46.70	39.90	43.50	47.45	49.20
400	32.98	34.83	37.80	39.10	32.98	36.45	39.60	40.70
500	15.85	16.87	19.30	16.50	15.85	18.10	20.24	17.10

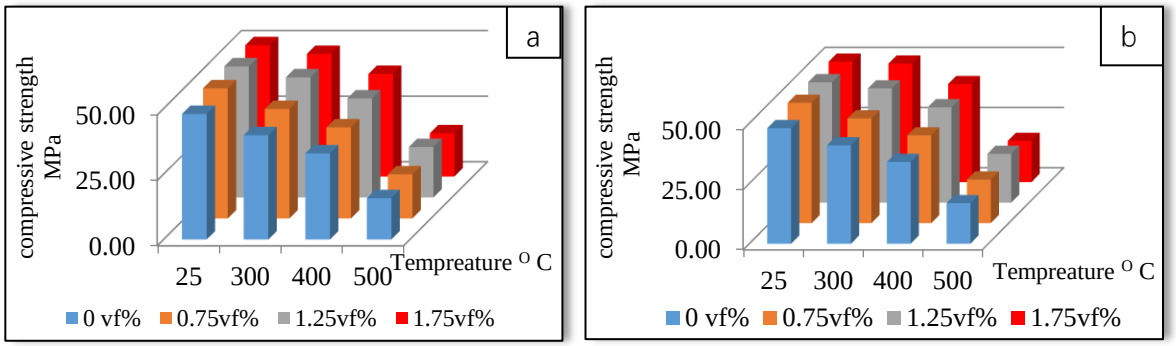

(a) Micro steel fiber (b) Hook steel fiber

Fig.9. Effect of burning temperatures and different V_f % on the compressive strength of SCC

The strength values ranged from 48 MPa to 55.87 MPa as the volume of hooked steel fibers increased. However, in the case of self-compacting concrete (SCC) specimens with micro steel fiber, this trend aligned with that of hooked steel fibers reaching to 53.4 MPa. When comparing the performance of both types of fibers, it is clearly visible that the SCC specimens with micro steel fibers were inferior in terms of compressive strength when compared to SCC specimens containing hook steel fibers. This is due to the better interlocking mechanism that hooked fibers have due to their deformed ends.

When subjected to fire flam with different temperatures, compressive strengths were reduced for all specimens with and without fiber as display in **Tab. 14** and **Fig. 10 (a, and b)** for both micro steel and hooked end fiber specimens.

Table 14. Reduction in compressive strength results at different burning temperatures using micro and hook steel fibers

Reduction in compressive strength (%)								
	Micro steel fiber				Hook steel fiber			
Temp. °C	MR	MS0.75	MS1.25	MS1.75	MR	MH0.75	MH1.25	MH1.75
300	16.88	15.81	13.19	12.55	14.80	14.10	12.52	11.94
400	31.28	29.91	28.41	26.78	29.20	28.02	26.99	27.15
500	66.98	66.06	63.45	69.10	73.17	72.60	70.39	76.75

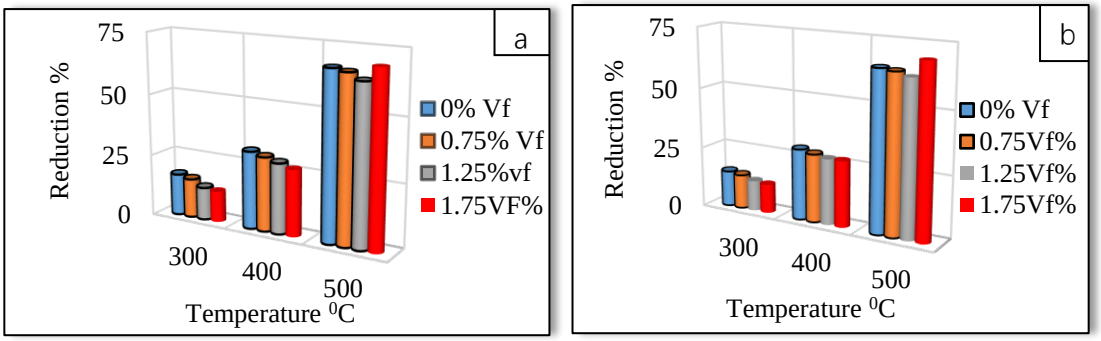

(a) Micro steel (b) Hook steel fiber

Fig.10 reduction percent of compressive strength for different V_f % and burning temperatures

Specimens that contain fibers (micro and hooked end steel fibers) experienced less reduction in compressive strength than specimens without steel fibers. Specimens with micro steel fibers experienced compressive strength lower than those of hooked steel fiber specimens. This is due to hooked-end fibers' better mechanical anchorage that provides a stronger bonding with the concrete matrix; hence, effectively arresting the growth of both micro and macro cracks during and after the burning process. After the samples were subjected to burning, a decrease in compressive strength values was observed with increasing burning temperatures from (300-500)ºC. This decrease diminishes with the addition of higher volumetric ratios of fibers, for both the hook and micro steel fibers used, compared to the same mixes at ambient temperature. When using a 1.75% ratio of hook fiber, a difference in this behavior was observed at 400 ºC and 500ºC, where the augment of reduction was (27.15, 69.39) % respectively. Moreover, when using 1.75% of micro fiber, the same behavior

was observed only at a burning temperature of 500 ºC, where it reached 69.10%. Adding 1.75% of hooked fibers reduce the workability of fresh concrete due to the non-uniform distribution of these fibers within the concrete matrix. When exposed to high burning temperatures above 400 ^{O} C, the efficiency of these fibers in bridging cracks decreases, and they lose part of their mechanical resistance at elevated burning temperatures. This results in a reduction in the efficiency of these fibers in improving properties at lower temperatures. Moreover, at high temperatures, damage may also arise due to the mismatch in thermal expansion between the steel fibers and the surrounding concrete matrix. Stress concentration at the fiber–matrix interface may result from differential thermal strain during heating because steel fibers have a higher coefficient of thermal expansion than concrete. This mechanism may enhance localized porosity surrounding the fibers and hasten the creation of micro cracks in the ITZ, and this is more clearly noticed for hook steel fiber than micro steel fiber at higher burning temperatures [48].

4.2.2 Splitting Tensile Strength

SCC specimens containing both types of fiber when tested for splitting tensile strength according to ASTM C496/C496M-17 [49], exhibited similar trends as compressive strength. **Tab. 15, Fig 11(a, and b)** displays the tensile strength results for samples with both types of fiber at ambient temperature and at different burning temperatures.

Table 15. Splitting tensile strength results at different burning temperatures using micro and hook steel fibers

Splitting tensile strength (MPa)								
	Micro steel fiber				Hook steel fiber			
Temp. ° C	MR	MS0.75	MS1.25	MS1.75	MR	MH0.75	MH1.25	MH1.75
25	3.29	3.89	4.30	4.50	3.29	4.46	4.98	5.52
300	2.88	3.50	3.94	4.20	2.88	3.95	4.45	5.03
400	2.51	3.10	3.58	3.83	2.51	3.43	3.90	4.21
500	1.31	1.80	2.12	1.78	1.31	1.96	2.38	2.12

Generally, splitting tensile strength increased with increasing the volume fraction of fiber in the mix. When comparing the performance of both types of fibers, there was no doubt that hooked fiber

specimens exhibited higher resilience to splitting tensile than those with micro steel fiber. Splitting tensile strengths ranged from 3.89 MPa to 4.50 MPa for specimens with micro steel fiber; however, readings ranging from 4.46 to 5.52 MPa were exhibited by SCC specimens with hooked steel fibers.

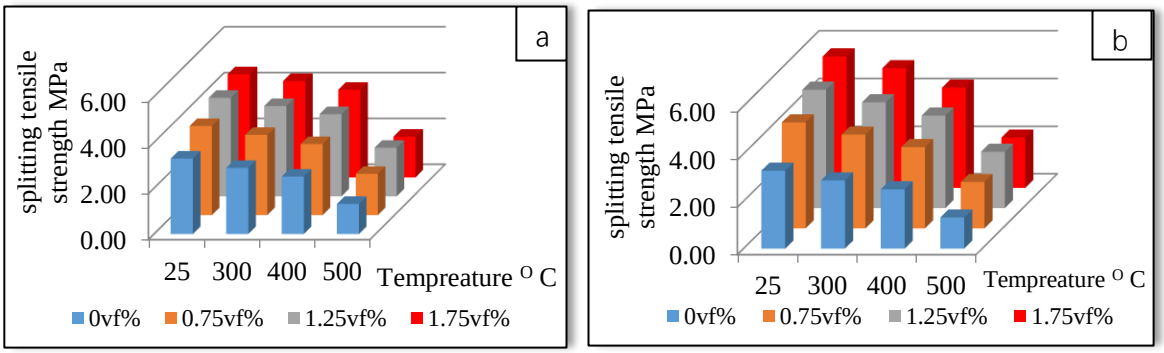

(a)Micro steel fiber (b) Hook steel fiber

Fig.11. Effect of burning temperatures and different Vf % on the splitting tensile strength of SCC

Similar to compressive strength, splitting tensile strength results decreased with increasing temperatures for all specimens with and without fiber addition. **Fig. 12 (a, and b) Tab. 16** lists the loss percentages in splitting tensile strengths for specimens with and without fiber at ambient and elevated temperatures.

Table 16. Reduction in splitting tensile strength results at different burning temperatures using micro and hook steel fiber

Reduction in splitting tensile strength (%)								
	Micro steel fiber				Hook steel fiber			
Temp. ºC	MR	MS0.75	MS1.25	MS1.75	MR	MH0.75	MH1.25	MH1.75
300	12.36	10.01	8.38	6.59	12.36	11.47	10.53	8.92
400	23.86	20.31	16.71	14.99	23.86	23.12	21.76	23.70
500	60.06	53.72	50.75	60.49	60.06	56.15	52.21	61.55

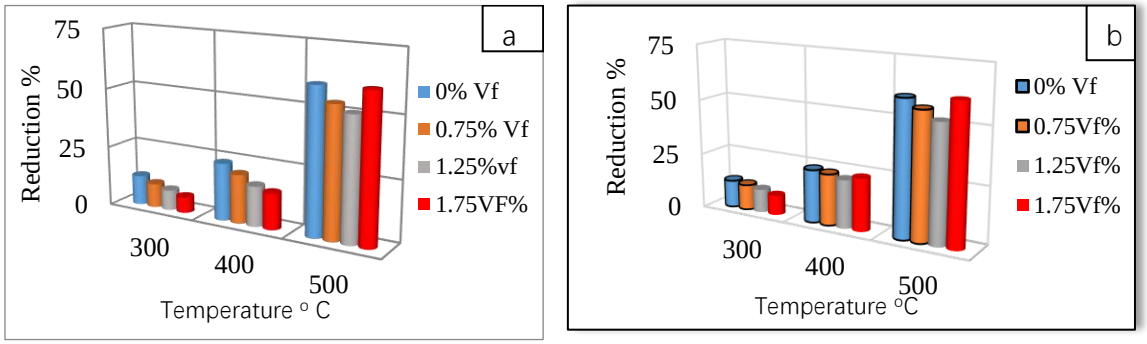

(a) Micro steel fiber (b) Hook steel fiber

Fig.12 reduction percent of splitting tensile strength for different V_f % and burning temperatures

With the elevation of temperatures, specimens without fibers exhibited strength loss higher than those contain steel fibers for all burning temperatures reaching to 60.06% at 500°C. Similarly to compressive strength, splitting tensile strength loss also increased. This is due to the degradation of the sample's matrix and possible de-bonding. When comparing splitting tensile strength loss of specimens containing fibers, hooked end fiber specimens showed higher losses in splitting tensile strengths than those containing micro-fibers. The losses in splitting tensile strengths reached to 23.70% and 61.55% for SCC samples containing 1.75% addition of hooked fibers when subjected to 400°C and 500°C, respectively. Whereas specimens having the same circumstances but with micro-steel fiber showed 14.99% and 60.49% splitting tensile strength loss for the same temperatures. This can be attributed to the behavior of both fibers when subjected to elevated burning temperatures. Micro steel fibers are less dependent on mechanical anchorage and have the tendency to distribute cracks evenly.

Unlike hook ended fibers are more reliant on bond and mechanical interlocking in which they deteriorate with increasing burning temperatures. Moreover the principal microstructural failure mechanisms of the fiber-matrix interface in fiber-reinforced concrete subjected to 500 °C include interfacial deboning caused by dehydration and thermal stresses, initiation of micro cracking in the Interfacial Transition Zone (ITZ), damage from differential thermal expansion, an increase in local porosity due to water evaporation, the formation of fiber pull-out channels, and localized matrix micro-spalling around fibers [50, 51].

4.2.3 Flexural Strength

Flexural strength was tested based on the specification ASTM C293/C293M-16 [52]. **Fig 13 (a, and b)** and **Tab. 17** illustrates the flexural strengths for both micro steel and hooked end fiber specimens at ambient and elevated temperatures.

Table 17. Flexural strength results at different burning temperatures using micro and hook steel fibers

Flexural strength (MPa)								
	Micro steel fiber				Hook steel fiber			
Temp. °C	MR	MS0.75	MS1.25	MS1.75	MR	MH0.75	MH1.25	MH1.75
25	4.78	5.72	6.23	6.61	4.78	6.20	6.82	7.36
300	3.95	4.93	5.47	5.84	3.95	5.21	5.80	6.32
400	3.34	4.10	4.65	4.97	3.34	4.41	4.90	5.15
500	1.80	2.35	2.90	2.34	1.80	2.53	3.30	2.56

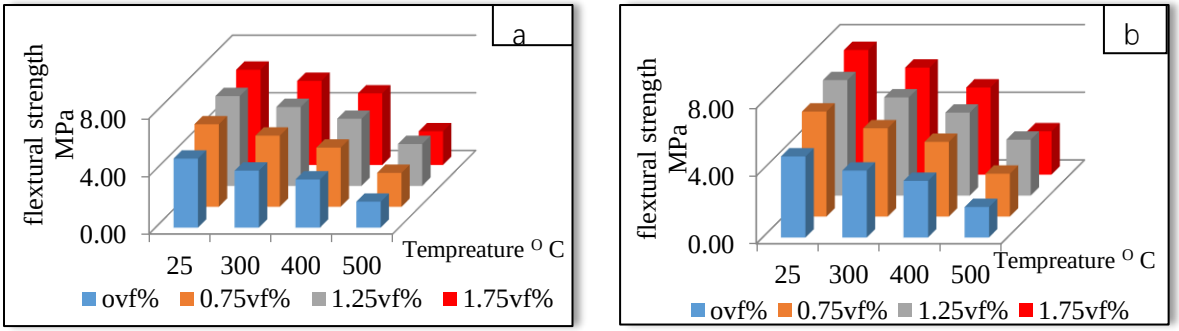

(a) Micro steel fiber (b) Hook steel fiber

Fig.13. Effect of burning temperatures and different V_f % on the flexural strength of SCC

In ambient temperatures, SCC specimens containing both types of fiber exhibited higher flexural strength readings than the control specimens. As expected, the increase in fiber addition increased the flexural strengths for both types of fiber. However, specimens containing hooked end steel fiber showed higher flexural strengths than those exhibited by specimens containing micro-steel fiber. Flexural strengths of hook-end fiber specimens ranged from 6.2 MPa at a fiber addition level of 0.75% to 7.36 at an addition level of 1.75%. Whereas the flexural strengths of specimens containing micro steel fiber were 5.72 MPa to 6.61 MPa at the same fiber addition levels mentioned above.

Fig. 14 (a, and b) and **Tab. 18** lists the flexural strength losses percentages for all specimens for micro steel and hooked end fibers respectively.

Table 18. Reduction in flexural strength results at different burning temperatures using micro and hook steel fibers

Reduction in flexural strength (%)								
	Micro steel fiber				Hook steel fiber			
Temp. °C	MR	MS0.75	MS1.25	MS1.75	MR	MH0.75	MH1.25	MH1.75
300	17.42	13.74	12.20	11.68	17.42	15.97	14.96	14.13
400	30.17	28.27	25.37	24.84	30.17	28.87	28.15	30.03
500	62.37	58.88	53.45	64.61	62.37	59.19	51.61	65.22

As a general observation, all specimens, with and without fiber, showed lower flexural strengths when subjected to elevated burning temperatures. The higher the temperature the higher the loss in

flexural strength when attempting a comparison for each specimen individually. However, a new rhythm was observed when comparing between specimens that have different fiber content. The loss of flexural strength was lower in the samples containing fiber addition ratios of 0.75%, 1.25%, and 1.75% compared to the same mix at ambient temperature, with improved behavior as the fiber volume ratio increased. This rhythm was seen with both micro and hooked end fibers at burning temperature of 300°C. At 500°C burning temperature, micro-fiber specimens containing 0.75 and 1.25 exhibited a flexural strength loss of 58.88% and 53.45% respectively in comparison to hook fiber 59.19% and 51.61%. Concerning 1.75% addition for hook steel fiber the reduction raises for both 400 and 500°C reaching to 30.03% and 65.22%, respectively compared to micro steel fiber which gained a reduction of 64.61% at 500°C only. The argument that the optimal fiber content 1.25% plays a huge role in toughness and in crack control for the two types of fiber used. The optimal fiber content creates a matrix where fibers are well distributed across the paste which effectively bridges cracks. In addition, it helps in delaying crack propagation in which the residual strength is increased. Furthermore, higher fiber content will lead in poor dispersion, clumping of fibers creating weak zones and micro-cracking under thermal stress due to fiber interaction. When there is no fiber, there is nothing to bridge or delay micro-cracking when it occurs.

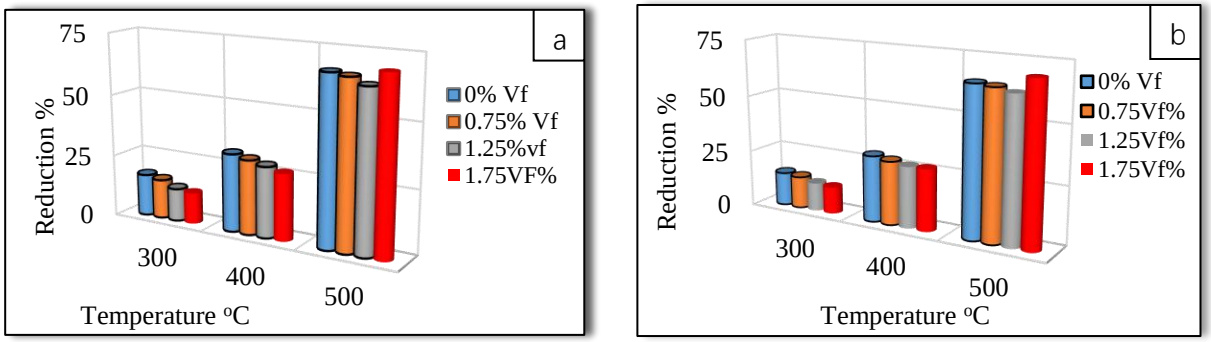

(a) Micro steel fiber (b) Hook steel fiber

Fig.14 reduction percent of flexural strength for different V_f % and burning temperatures

5 Correlations

The effect of elevated burning temperatures, fiber type and fiber addition on properties of SCC concrete samples is analyzed. It is worth mentioning that all burnt samples were gradually cooled and brought to room temperature then were tested for their mechanical properties. As a general observation, compressive strength decreases with an increase in burning temperature. However, type of fiber also affects the performance of SCC samples when subjected to elevated temperatures. **Tab.19** and **Fig.15** lists the R^2 values and equations for compressive strength plotted against temperature for different types of fiber and increasing fiber addition.

Table 19. R^2 values and equations between compressive strength and temperature

Fiber addition%	Fiber type	equation	R^2
0.75	Micro steel	$Y = -0.0002x2 + 0.0492x + 48.445$	0.9876
	Hooked end	$Y = -0.0002x2 + 0.0554x + 49.235$	0.9870
1.25	Micro steel	$Y = -0.0002x2 + 0.0584x + 51.352$	0.9913
	Hooked end	$Y = -0.0003x2 + 0.0633x + 52.655$	0.989
1.75	Micro steel	$Y = -0.0003x2 + 0.079x + 51.38$	0.9843
	Hooked end	$Y = -0.0003x2 + 0.0851x + 53.718$	0.9814

A linear regression model accounted for 70% of the data's variance (R^2 =0.7). A non-linear alternative was selected due to its superior predictive power, explaining 98% of the variance (R^2 =0.98) due to its more accurate framework for characterizing the relationship between the variables. R^2 values range between (0.9814 and 0.9913) suggesting that the correlation between compressive strength, fiber type and temperature is strong and far from random. It is important to note that R^2 values for micro steel SCC specimens are higher than those exhibited by hooked end SCC specimens. This is due to the more consistent and predictable way that micro steel fibers vary with temperature

than that of SCC specimens containing hooked end fiber. It can be reasoned to micro-steel's better consistency in dispersion because of their shorter and finer nature, they tend to disperse more uniformly leading to fewer voids and weak zones and behave more homogeneously when subjected to heat. In other words, as temperature rises, specimens containing micro-steel fiber lose strength following a smoother, more linear pattern; hence, the high regression fit.

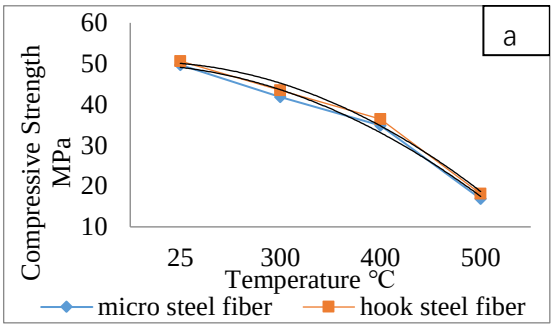

(a) 0.75 V_f % for micro and hook steel fiber

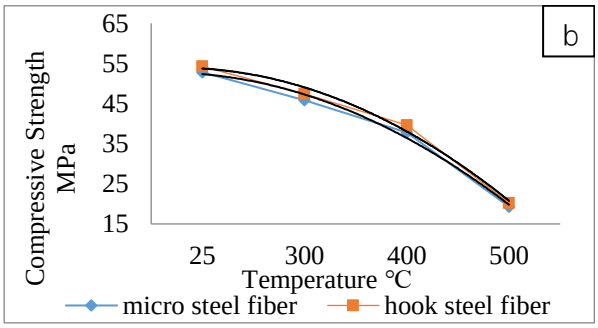

(b) 1.25 V_f % for micro and hook steel fiber

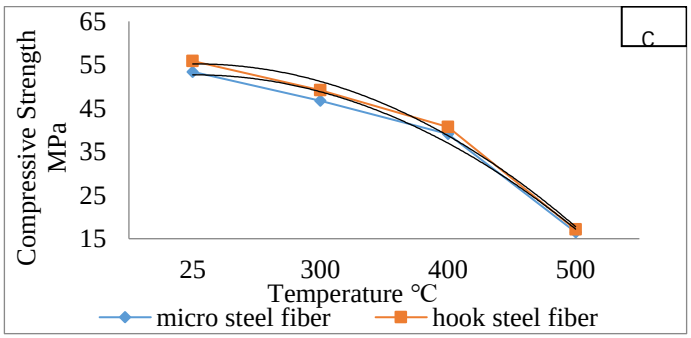

(c) 1.75 V_f % for micro and hook steel fiber

Fig.15 correlation between compressive strength and burning temperatures

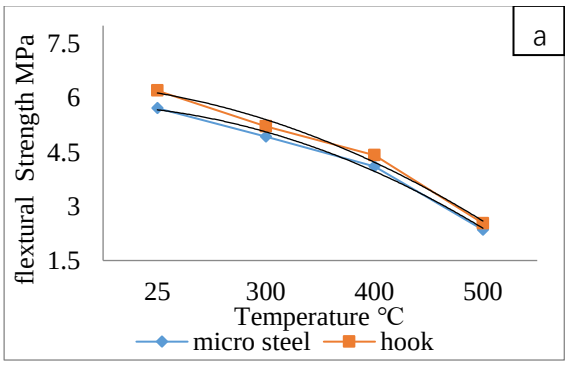

(a) 0.75 V_f % for micro and hook steel fiber

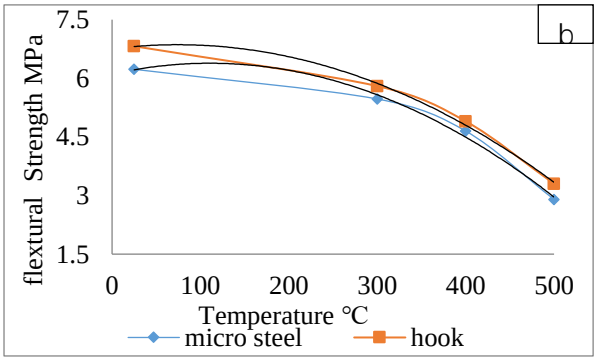

(b) 1.25 V_f % for micro and hook steel fiber

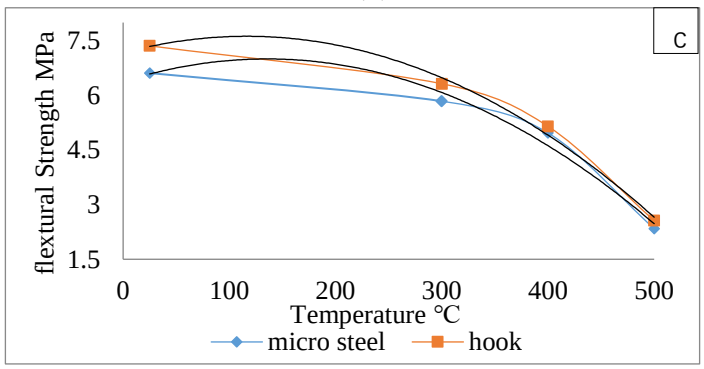

(c) 1.75 V_f % for micro and hook steel fiber

Fig.16 correlation between flexural strength and burning temperatures:

Tab. 20 and **Fig.16** shows the R^2 values and the best fit correlation equations between flexural strength readings and temperature. When observing the correlations between flexural strength readings, fiber type and temperature, a different rhythm arises. As the proportion of fiber increases (>0.75%), hook end fiber samples show higher R^2 readings than those of micro-steel fiber. This is an indication that the data of micro-steel SCC specimens show a more scattered trend. This could be reasoned to the stronger anchorage of hooked end fiber has with the matrix of the SCC sample. When cracking propagates, more hooked end fibers engage providing constant bridging, delaying crack width propogation leading to an increase in flexural strength. Unlike hooked end fibers, micro steel fiber behaves in a different manner. As micro-steel fiber content increases, nonlinear behavior in flexural strength is exhibited. High quantity of micro-steel fiber in SCC causes an increased number of voids within the matrix. This causes the increase in flexural strength to be less uniform; hence, reducing the R2 values

Table 20. R^2 values and equations between flexural strength and temperature

Fiber addition%	Fiber type	equation	R^2
0.75	Micro steel	$Y = -2E-05X2 + 0.0049X + 5.59$	0.9939
	Hooked end	$Y = -2E-05X2 + 0.0043X + 6.0918$	0.9906
1.25	Micro steel	$Y = -2E-05X2 + 0.005X + 6.1074$	0.9936
	Hooked end	$Y = -2E-05X2 + 0.0029X + 6.7525$	0.9975
1.75	Micro steel	$Y = -3E-05X2 + 0.0092X + 6.3764$	0.9807
	Hooked end	$Y = -3E-05X2 + 0.0079X + 7.1662$	0.9926

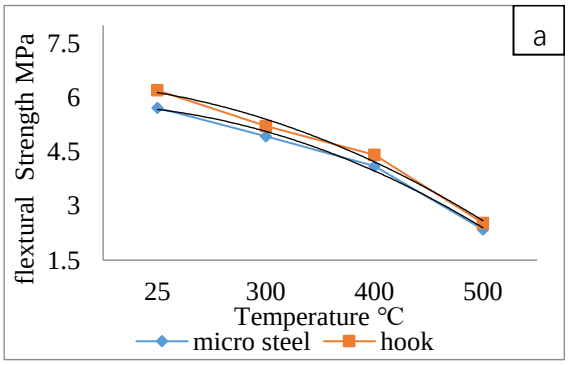

(a) 0.75 V_f % for micro and hook steel fiber

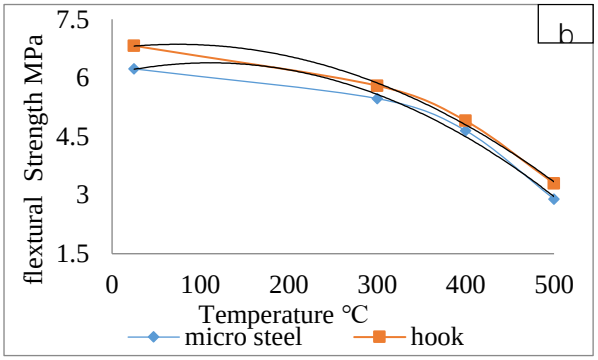

(b) 1.25 V_f % for micro and hook steel fiber

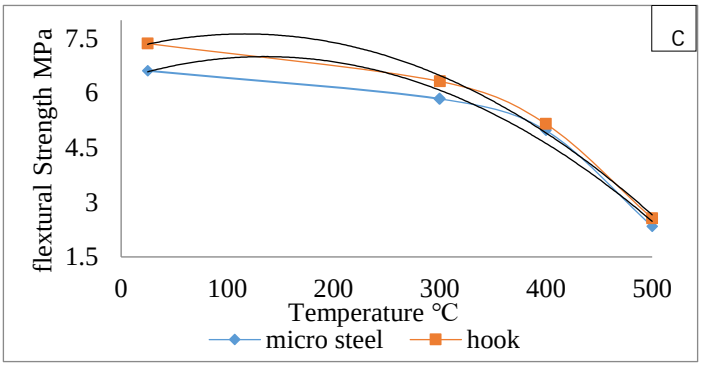

(c) 1.75 V_f % for micro and hook steel fiber

Fig.16 correlation between flexural strength and burning temperatures

Tab.21 lists the R^2 values and equations conceived by correlating splitting tensile strength and burning temperature at the age of 56 days. **Fig.17** shows the correlation between these two properties at the same age. It is obvious that hooked end SCC samples showed higher R^2 values than those obtained from micro-steel SCC samples. In other words, the splitting tensile strength reduction followed a predictable and more consistent pattern in comparison to that of the SCC samples

containing micro-steel fiber. This can be reasoned to fiber geometry, thermal degradation behavior and homogeneity. Mechanical anchorage provided by hooked end fibers improves bond strength between the fibers and the mix matrix, and as temperature rises it results in an even stress-strain response. At elevated temperatures, deterioration of paste microstructure occurs. This where the hooked end fibers show superior crack bridging ability for a longer duration causing smooth and constant strength loss in comparison to micro-steel fibers. Furthermore, hooked end fibers tend to limit localized damage and have the ability to distribute stress more in a more efficient manner.

Table 21. R^2 values and equations between splitting tensile strength and temperature

Fiber addition%	Fiber type	equation	R^2
0.75	Micro steel	$Y = -2E-05x2 + 0.0045x + 3.7745$	0.9775
	Hooked end	$Y = -2E-5x2 + 0.0047x + 4.3427$	0.9836
1.25	Micro steel	$Y = -2E-05x2 + 0.0054x + 4.1595$	0.9852
	Hooked end	$Y = -2E-05x2 + 0.0054x + 4.1595$	0.9666
1.75	Micro steel	$Y = -3E-05x2 + 0.0085x + 4.2743$	0.9498
	Hooked end	$Y = -3E-05x2 + 0.0082x + 5.3157$	0.9876

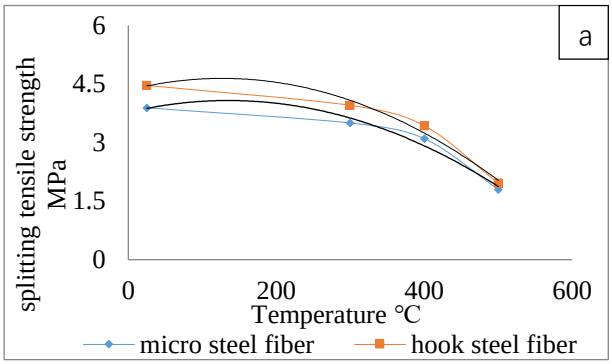

(a) 0.75 V_f % for micro and hook steel fiber

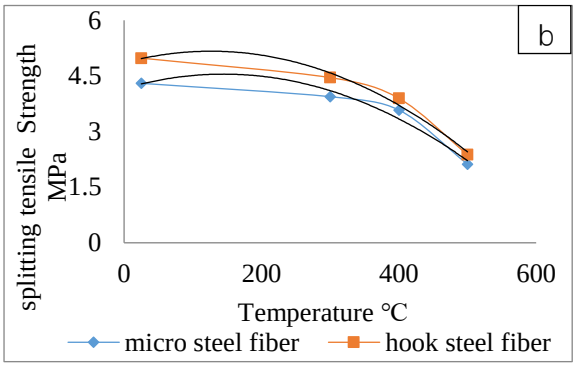

(b) 1.25 V_f % for micro and hook steel fiber

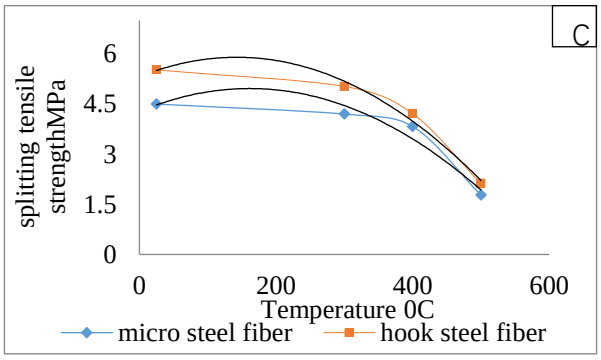

(c) 1.75 V_f % for micro and hook steel fiber

6 Statistical Conjectures

For the sake of quantitatively assessing the performance of the concrete samples with different types of fiber subjected to different temperatures was meaningful from a statistical perspective, a two-factor analysis of variance (ANOVA) without replication was conducted for all investigated properties, putting into consideration fiber dosage (0% -1.75%) and burning temperatures (25°C-500°C) as independent variables. The null hypothesis suggests that there are no performance differences shown by the concrete samples regardless of fiber dosage volumes and burning temperatures. A confidence level of 95% ($\alpha = 0.05$) was adopted, where a statistically significant effect is indicated through a p-value less than 0.05.

Tab.22 above shows that both temperature and dosage level have significant impact on the performance parameters namely (compressive, flexural and tensile strengths) regardless of fiber type.

Although both types of fiber show significant differences, p-values for specimens containing micro-steel fiber are slightly lower than those of hook-ended specimens through all performance parameters. This indicates that concrete specimens containing micro-steel fiber show higher sensitivity to temperature and dosage changes than those containing hook-ended fiber. The F-critical value for all performance parameters and for both types of fiber is equal to 3.862. The f-statistics values show that temperature is more significant than fiber dosage when observing their effect on compressive strength. However, fibre dosage is much more critical for tensile strength.

Table 22. Summary of two-factor ANOVA results

Performance parameter	Type of fiber	Source of variation	P-value	F-statistic	Significant difference Yes/no
Compressive strength	Micro-steel	Temperature	9.8E-10	368.7026	yes
		Dosage level	0.0023	10.89855	yes
	Hook-ended	Temperature	1.3E-09	342.7194	yes
		Dosage level	0.0008	14.72618	yes
Flexural strength	Micro-steel	Temperature	2.8 E-07	102.6029	yes
		Dosage level	0.001	13.68819	yes
	Hook-ended	Temperature	5.9E-07	86.87023	yes
		Dosage level	0.0001	24.82781	yes
Tensile strength	Micro-steel	Temperature	2.1E-07	110.0000	yes
		Dosage level	6.2E-05	28.60000	yes
	Hook-ended	Temperature	8.7E-07	79.01958332	yes
		Dosage level	2.4E-07	36.06923176	yes

Tab.23 lists the mean, SD and CV% for the performance parameters at different burning temperatures and fiber types.

Table 23. Statistical analysis

parameter	Temperature	mean		SD		CV%	
Compressive strength	°C	micro	hook	micro	hook	micro	hook
	25	50.975	52.188	2.562	3.545	5.025	6.793
	300	44.0675	45.013	3.954	4.159	8.972	9.241
	400	36.178	37.433	2.782	3.472	7.689	9.275
	500	17.13	17.823	1.507	1.856	8.797	10.414
Flexural strength	°C	micro	hook	micro	hook	micro	hook
	25	5.835	6.291	0.792	1.111	13.568	17.666
	300	5.048	5.298	0.822	0.991	16.277	18.704
	400	4.265	4.450	0.714	0.801	16.734	18.007
	500	2.348	2.548	0.449	0.613	19.131	24.043
Tensile strength	°C	micro	hook	micro	hook	micro	hook
	25	3.995	4.563	0.534	0.952	13.372	20.873
	300	3.630	4.077	0.577	0.912	15.908	22.371
	400	3.255	3.49	0.582	0.746	17.873	21.374
	500	1.775	1.965	0.368	0.470	20.728	23.893

The in-depth statistical analysis shown in the table above sets a firm conclusion that a massive drop in strength is observed at the 500°C. The compressive strength drops about 30% when temperature is increased from 25°C to 400°C while strength plummets by over 50% when temperature is increased from 400°C to 500°C in comparison to micro steel fiber, the results also show that hook ended fibers show a consistent superior behavior in which a higher mean is observed. Due to concrete's nature, compressive strength has a relatively low CV% (roughly 5-10%) in comparison to flexural and tensile strengths where a higher CV% was observed. Furthermore, CV% increased as the temperature rises to 500°C. in addition, specimens containing hook ended fiber show a higher mean (higher strength), but micro-steel specimens were observed to show higher consistency (lower CV%).

7 Conclusions

- The workability of self-compacting concrete declines with the increase in the volume fraction

of steel fibers for both types used.

- The use of hook steel fiber had a greater impact on workability than micro steel fiber.
- The compressive, flexural, and splitting tensile strength were improved by increasing the percentage of added fibers, and the rate of increase for flexural and splitting was much higher than for the compressive strength.
- The percentage increase for all hard properties was higher when using hook steel fibers compared to micro steel fibers.
- When samples are exposed to burning, the hardened properties values generally decline with increasing burning temperatures.
- The presence of fibers helped to reduce the rates of SCC impact after exposure to different temperatures, as it reduced the percentage reductions for all hardened properties.
- This enhancement was directly proportional to the augmentation of fiber volume fraction for both types; except for 1.75% hook steel fiber at 400 and 500 ºC burning temperatures, where there was a decrease in the improvement rates. Moreover, as for 1.75% micro steel fibers, this behavior was observed at 500 ºC only.
- At 300 ºC burning temperature, 1.75% was the best V_f for both types used.
- At 400 ºC burning temperature, 1.75% was the best V_f for micro steel fiber, and 1.25% was the optimal V_f for hook steel fiber.
- At 500 ºC burning temperature, 1.25% was the optimal V_f for both types used.

8 Recommendations

A section for the proposed recommendations was added after the conclusions section.

- Conducting a Scanning Electron Microscopy (SEM) examination SEM (Microscopy), FTIR (Fourier-Transform Infrared Spectroscopy) , and X-ray CT (Computed Tomography).
- Burning at temperatures above 500°C and studying the effect of very high temperatures on concrete behavior.
- Using more than one type of extinguishing method, such as gradual and sudden, and their impact on the properties of concrete.
- Using polypropylene fibers as hybrid fibers with steel fibers.
- Using hybrid fibers of both types in the same mix.
- Studying additional properties such as the modulus of elasticity, load-deflection curve, and absorbed energy.
- investigating the pull-out behavior or bond-slip relationship between fibers and concrete.

Acknowledgement

The authors would like to express their gratitude to the University of Baghdad, and especially the College of Engineering/ Civil Engineering Department, for the support they provided during the practical part of the research, including the provision of all the necessary equipment and furnaces for the firing process to fulfill the requirements of this research.

References

[1] Qin D, Gao P, Aslam F, Sufian M, Alabduljabbar H. A comprehensive review on fire damage assessment of reinforced concrete structures. Case Studies in Construction Materials 2022; 16: https://doi:10.1016/j.cscm.2021.e00843.

[2] Bakhtiyari S, Allahverdi A, Rais-Ghasemi M. A case study on modifying the fire resistance of self-compacting concrete with expanded perlite aggregate and zeolite powder additives. Asian Journal of Civil Engineering 2014; 15(3): 339-349. https://www.researchgate.net/publication/286147375.

[3] Ghanim HH, Awad H K. Effect of (LECA) as a Partial Replacement on Some Properties of Glass Fiber Reinforced Self-Compacting Concrete Exposed to Fire Flame. IOP Conference Series: Earth and Environmental Science 2024; 1374(1): https://doi:10.1088/1755-1315/1374/1/012076.

[4] Aslani F, Hamidi F, M.a Q. Fire Performance of Heavyweight Self-Compacting Concrete and Heavyweight High Strength Concrete. School of Civil Environmental and Mining Engineering, University of Western

Australia 2019; 822 (12): https://doi:10.3390/ma12050822.
[5] Ryu E, Shin Y, and Kim H. Effect of Loading and Beam Sizes on the Structural Behaviors of Reinforced Concrete Beams Under and After Fire. International Journal of Concrete Structures and Materials 2018; 12(54): https://doi:org/10.1186/s40069-018-0280-5.
[6] Aboud R K, Awad H K, Mohammed Sh D .Effect of Fire Exposure on the Properties of Self-Compacting Concrete reinforced by Glass Fibers. Engineering, Technology & Applied Science Research 2024; 14(2): 13369-13375. https://doi.org/10.48084/etasr.6924.
[7] Kodur V. Properties of concrete at elevated temperatures. Hindawi Publishing Corporation ISRN Civil Engineering 2014; 2014: Article ID 468510. https://doi.org/10.1155/2014/468510.
[8] Mathews M K, Kiran T, Nammalvar A, Andrushia A D, Alengaram U J. Efficacy of Fire Protection Techniques on Impact Resistance of Self-Compacting Concrete Buildings 2023; 1487(13): https:// doi:org/ 10.3390/buildings13061487.
[9] Ali E M , Adheem A H, and Naje A S. Fire Flame Effect on The Strength of Self –Compacting Concrete. Al Muthanna journal for engineering science 2013; 2(1): https://doi:10.52113/3/eng/mjet/2013(02)01/01 -13.
[10] Noumowé A, Carré H, Daoud A, Toutanji H. High-Strength Self-Compacting Concrete Exposed to Fire Test. Journal of Materials in Civil Engineering 2006; 18(6) : 754-758. https://doi:10.1061/(ASCE)0899-156 1(2006)18:6(754).
[11] Muhammad A, Usman N, Gambo N. Effect of binary blended pozzolanic materials on properties of self-compacting concrete. International Journal of Construction Management 2022; 22(7): 1323–1332. http s://doi: 10.1080/15623599.2019.1707500.
[12] Heiza K M. Performance of Self-Compacted Concrete Exposed to Fire or Aggressive Media. Concrete Research Letters 2012; 3(2). https://www.challengejournal.com/index.php/cjcrl/article/view/147/110.
[13] Olafusi O , Adewuyi A , Otunla A, Babalola A . Evaluation of Fresh and Hardened Properties of Self-Compacting Concrete. Open Journal of Civil Engineering 2015; 5(1): https://doi.org/10.4236/jce.2015. o51 001.
[14] Karem N A M, Awad H K. Basalt Fiber Implication on Fresh and Mechanical Properties of Self-Compacting Concrete. Engineering, Technology & Applied Science Research 2025; 15(4): 24637-246 43. https://doi: https://doi.org/10.48084/etasr.11411.
[15] Motar S B, Awad H K. Behavior of Steel-Fiber Reinforced Lightweight Self-compacting Concrete Containing LECA after the Exposure to Internal Sulfate Attack. E3S Web of Conferences 2023; 427: 02007 . https:// doi.org/10.1051/e3sconf/202342702007.
[16] Saadoon T D, Obaidi H, Dulaimi A, Ghiassi B. Modeling performance of different sustainable self-compacting concrete pavement types utilizing various sample geometries. Open Engineering 2025; 15: 20250117. https://doi.org/10.1515/eng-2025-0117.
[17] Ali H H, Awad H K. The Influence of Nano-Silica on Some Properties of Light Weight Self-Compacting Concrete Aggregate. E3S Web of Conferences 2023; 427(8): 02008. https://doi.10.1051/e3sconf/20234270 2008.
[18] Oztekin E, Kina C,and Turk K. Effect of Micro Fiber Content on Workability of Self-compacting Concrete. Conference: 13th International Congress on Advances in Civil Engineering (ACE 2018); September 2018: https://www.researchgate.net/publication/330669217.
[19] Naeem B K, Awad H K. Investigation of properties of SCC with perlite as a partial replacement of coarse and fine aggregate. IOP Conference Series: Earth and Environmental Science.2024; 1374(1). 012013. https: //doi.org/10.1088/1755-1315/1374/1/012013.
[20] Aboud R K, Awad H K, Mohammed S D. Fire flame effect on the compressive strength of reactive powder concrete using different methods of cooling, IOP Conf. Series: Materials Science and Engineering (518) 2019; 022029: https://doi:10.1088/1757-899X/518/2/022029.
[21] Ning, X, Wang, Y, and Zhu J. Effects of Different Fibers on Mechanical Properties and Fire Resistance of Self-Compacting Concrete. Applied Sciences 2022; 12(24): 12779. https://doi.org/10.3390/app122412779.
[22] Banthia N, Krstulovic-Opara N, Galinat M A. ACI 544.5R-10. Report on the Physical Properties and Durability of Fiber-Reinforced Concrete; American Concrete Institute, Chapter 3 2010; https://www.concre te.org/Portals/0/Files/PDF/Previews/544.5R-10web.pdf.
[23] Yang Q, Wang H, Zeng L, Guan L, Cheng J , Xiang R. Properties of High-Content Micro-Steel Fiber Self-Compacting Concrete Incorporating Fly Ash and Slag Powder Performance Study. Contraction Materials 2023; 3(4): 558–575. https://doi.org/10.3390/constrmater3040035.
[24] Iqbala S, Alia A, Holschemachera K, Bierb T A. Effect of change in micro steel fiber content on properties of High strength Steel fiber reinforced Lightweight Self-Compacting Concrete (HSLSCC). Conference Paper in Procedia Engineering · Procedia Engineering. 2015; 122: 88–94. https://doi.10.1016/j.proeng.2015 .10.011.
[25] Ashteyata A, Obaidatc A, Kharabshehd T, Harahshehb A. Flexural behavior of high-strength reinforced concrete beam with hybrid fiber under normal and high temperature. Sustainable Structures.2024; 4(2):

000051. https://doi: 10.54113/j.sust.2024.000051.
[26] Ali S M, Awad H K. The Effect of Hybrid Fibers on Some Properties of Structural Lightweight Self-Compacting Concrete by using LECA as Partial Replacement of Coarse Aggregate. Engineering, Technology & Applied Science Research 2024; 14(4): 15002-15007. https://doi.org/10.48084/etasr.7425.
[27] Gu Z, Feng H, Gao D, Zhao J, Wei C, Wu C. Fatigue behavior and calculation methods of high strength steel fiber reinforced concrete beam. Sustainable Structures 2023; 3(2): 000028. https://doi.10.54113/j.sust.2023.000028.
[28] Kalifa P, Chéné G, Galle C. High-temperature behaviour of HPC with polypropylene fibers. From spalling to microstructure. Applied Sciences 2001; 31(10): 1487-1499. https://doi:10.1016/S0008-8846(01)00596-8
[29] Al-Kab W H, Awad H K. Fire flame effect on some properties of hybrid fiber reinforced LECA lightweight self-compacting concrete. Magazine of Civil Engineering 2024; 17(5): Article No.12806. https://doi.10.34910/MCE.128.6.
[30] Karim M M. Effect of Fire Flame Exposure on some Properties of Fiber Reinforced High Strength Concrete. Journal of Babylon University/Pure and Applied Sciences 2011; 19(3). 1184-1197.
[31] Wang W, Zhang Y, Mo Z, Wei H. Study on impact resistance of steel fiber reinforced concrete after exposure to fire. High Temperature Materials and Processes 2024; 43(1). https://doi.org/10.1515/htmp-2024-0021.
[32] Abbas A M, Alwash J J. Comparative Performance of SF, PPF and Hybrid Fiber-Reinforced Self-Compacting Lightweight Concrete Under Fire Exposure. International Information and Engineering technology Association 2023; 47(4). 237-245. https://doi.org/10.18280/acsm.470406.
[33] Awad H K. Influence of Cooling Methods on the Behavior of Reactive Powder Concrete Exposed to Fire Flame Effect. Fibers 2020; 8(3), 19. https://doi.org/10.3390/fib8030019.
[34] IQS. No. 5-2019. Iraqi standard specification for Portland Cement. Baghdad, Iraq. Central Agency for Standardization and Quality Control.2019.
[35] ASTM C150/C150M-20. Standard Specification for Portland Cement. American Society for Testing and Materials, 2020. https://store.astm.org/c0150_c0150m-20.html.
[36] IQS.No. 45-1984. Iraqi Specification for Aggregate from Natural Sources for Concrete and Building Construction. Baghdad, Iraq: Central Agency for Standardization and Quality Control. 1984.
[37] ASTM C33/C33M-18: Standard Specification for Concrete Aggregates. American Society for Testing and Materials; 2018. https://store.astm.org/c0033_c0033m-18.
[38] ASTM C1240-20 Standard Specification for Silica Fume Used in Cementitious Mixtures. West Conshohocken, PA, USA. American Society for Testing and Materials; 2020. https://store.astmorg/c1240-20.html.
[39] ASTM C494/C494M-17 Standard Specification for Chemical Admixtures for Concrete 2017; https://storeastm.org/c0494_c0494m-17.html.
[40] The European Guidelines for Self-Compacting Concrete Specification, Production and Use ‘The European Guidelines for Self Compacting Concre 2005; https://www.theconcreteinitiative.eu/images/ECP_Documents/EuropeanGuidelinesSelfCompactingConcrete.pdf.
[41] Ahmad J, Zhou Z, Deifalla A F. Steel Fiber Reinforced Self-Compacting Concrete: A Comprehensive Review. International Journal of Concrete Structures and Materials 2023; 17: Article number 51. https://doi:10.1186/s40069-023-00602-7.
[42] Aslani F, Hamidi F, Ma Q. Fire performance of heavyweight self-compacting concrete and heavyweight high strength concrete. Materials 2019; 12 (5): https://doi.10.3390/MA12050822.
[43] Mathews M E, Kiran T, Nammalvar A, Andrushia A D, Alengaram U J. Efficacy of Fire Protection Techniques on Impact Resistance of Self-Compacting Concrete. Buildings Jun 2023; 13 (6): https://doi10.3390/buildings13061487.
[44] Agwa I S, Abdelsalam B A, Abdel Hafezl R D, Abd-Al Ftah R O. Behavior of eco-friendly concrete reinforced with hybrid recycled fibers. Sustainable Structures. SUST. 2025; 5(1): https://doi.10.54113/j.sust.2025.000064.
[45] ASTM C192/C192M-24: Standard Specification for Concrete Aggregates." American Society for Testing and Materials, 2024. https://store.astm.org/c0192_c0192m-19.html.
[46] ASTM E119-20. Standard Test Methods for Fire Tests of Building Construction and Materials. American Society for Testing and Materials 2020; https://store.astm.org/e0119-20.html.
[47] BS EN 12390-3:2019. Testing hardened concrete – Compressive strength of test specimens. London, UK: BSI, 2019. https://www.standards.govt.nz/shop/bs-en-12390-32019.
[48] Liu y L, Wu K, Qian L P, Wang Y, Guo D. Effect of polyethylene glycol (PEG) modification on strength and microstructure of geopolymer paste. Construction and Building Materials 2025; 489: Article No. 142378. https://doi.org/10.1016/j.conbuildmat.2025.142378.
[49] ASTM C496/C496M-17. Standard Test Method for Splitting Tensile Strength of Cylindrical Concrete Specimens. American Society for Testing and Material. 2017. https://store.astm.org/c0496_c0496m-17.htm

l.

[50] Liu Y, Liu C, Qian L, Wang A , Sun D, Guo D. Foaming processes and properties of geopolymer foam concrete: Effect of the activator. Construction and Building Materials 2025; 391: Article No. 131830. https://doi.org/10.1016/j.conbuildmat.2023.131830.

[51] Guo D, Zhu M, Deng J, Zhong M, Zhou H. A novel methodology for determining the FRP-to-steel/concrete bond-slip relationship from load-displacement curves under thermal effects. Composite Structures 2026; 377: Article No. 119886. https://doi.org/10.1016/j.compstruct.2025.119886.

[52] ASTM C293/C293M-16. Standard Test Method for Flexural Strength of Concrete (Using simple beam with center point loading). American Society for Testing and Materials 2016. https://store.astm.org/c0293_c0293m-16.html.